Antiphase synchronization of electrically shaken conducting beads

E. Mersch and N. Vandewalle
Group for Research and Applications in Statistical Physics, Institut de Physique B5, Université de Liège, B-4000 Liège, Belgium
(Received 21 December 2010; revised manuscript received 20 October 2011; published 1 December 2011)

When a spherical conducting bead is placed in an electrode, it experiences an electric force. In a plane capacitor, it can undergo a periodic bouncing between the electrodes. Using a fast video camera, we measured the acceleration of the bead and the period of its motion as a function of the applied voltage. A mathematical model based on the hypothesis of electrostatic equilibrium is proposed to describe the dynamics of the system. We observe a stabilization of the trajectories: A bead bouncing between two electrodes tends to oscillate on a quasivertical trajectory, whatever its initial horizontal velocity. When two identical beads are placed together in a capacitor, they oscillate at the same frequency and an antiphase synchronization effect occurs. We propose a simple mechanism based on a Kuramoto-like model to explain it.

DOI: 10.1103/PhysRevE.84.061301 PACS number(s): 45.70.−n, 45.50.−j, 05.45.Xt, 41.20.Cv

I. INTRODUCTION

When micrometer- or millimeter-sized objects are placed in contact with an electrode, they can experience forces greater than their weight. The dynamics of a conducting bead immersed in a poorly conducting liquid inside a horizontal plane capacitor submitted to a dc voltage was studied by Khayari *et al.* [1]. When charged on the bottom plate, the ball is pushed upward. After its discharge through the liquid, it goes back down to the bottom electrode because of gravity. The system exhibits a periodic dynamics. The same experiment was conducted with an additional alternating electric field [2]. When increasing the amplitude of the alternating electric field, the system exhibits a period-doubling bifurcation analogous to the one observed for a ball mechanically shaken on a horizontal plate.

For a larger number of particles, the mutual interactions are responsible for some fascinating collective behaviors. Saint Jean and co-workers studied the diffusion of millimeter-sized spherical conducting particles placed between electrodes of different geometries and submitted to a mechanical shaking. They used this system to study the structure and the melting of small Wigner crystals in two dimensions [3–7]. They also studied the single-file diffusion problem within this system [8–10]. Aranson and co-workers [11–19] studied some collective behaviors of large assemblies of conducting beads and glass beads of various diameters enclosed in plane capacitors. They studied the formation dynamics of clusters and could apply the attachment-detachment-controlled Ostwald ripening theory to describe it [11–15]. They studied the velocity distributions of this far from equilibrium system [16] as well as some pattern formation when micrometer-sized conducting spheres are immersed in a poorly conducting liquids in the presence of a dc electric field [17–19]. Zhang and Liu studied the effect of an alternating electric field on a very similar experiment [20].

In this work we focus our attention on a minimalist version of the experiment of Aranson and co-workers. We study the behavior of a single, two, or three spherical conducting beads submitted to a constant and homogeneous electric field. In Sec. II we describe our experimental setup. Section III is dedicated to the problem of a single bead. In Sec. IV we discuss the dynamics of two interacting beads.

II. EXPERIMENTAL SETUP

A sketch of our experimental setup is shown in Fig. 1. One, two, or three spherical beads are placed between two horizontal plane electrodes. For the experiments conducted with a single bead, we used two glass beads with respective diameters $d = 400$ and 488 μm coated with a conducting layer as well as a steel bead of diameter $d = 500$ μm. For the experiment with two or three beads we used two stainless steel beads with a diameter $d = 2$ mm. The plates of the capacitor are two parallel squares with an edge $D = 60$ mm separated by a fixed gap $h = 3$ mm. A dc voltage V comprised between 0 and 5000 V is applied to the electrodes. The cell is open in an atmosphere of controlled humidity (43% relative humidity) at ambient pressure and temperature. The choice of this humidity is motivated by a recent work [21] demonstrating a minimum of bead-bead cohesion induced by capillary condensation when relative humidity is approximately equal to 40–50%. A fast CCD camera records the trajectory from the side at a frame rate ranging between 500 and 6000 fps.

III. DYNAMICS OF A SINGLE BEAD

A. Experimental results

At the beginning of the experiment, the bead is placed in contact with the bottom electrode. If the applied electric field is large enough, the particle can detach and accelerate in the direction of the upper electrode. It collides with this electrode. During the bouncing, the bead charges with the opposite sign and it further accelerates in the opposite direction. A periodic motion with a limit cycle is thus reached. Figure 2 represents the vertical coordinate z of a 488-μm coated glass bead as a function of time t. The applied voltage V is 2000 V and the frame rate is 6000 fps. The limit cycle is reached after about ten collisions, which correspond to 50 ms.

We recorded the trajectories of a single 400-μm coated glass bead. We measured its acceleration for different voltage values. We obtained the acceleration a due to the electric force by subtracting the gravitational acceleration $g = 9.81$ m s^{-2}. Figure 3 shows the acceleration a as a function of the applied voltage V. Each dot is an average of five samples. The acceleration increases with the voltage V in a quadratic way (see the model in Sec. III B). The acceleration a reaches values

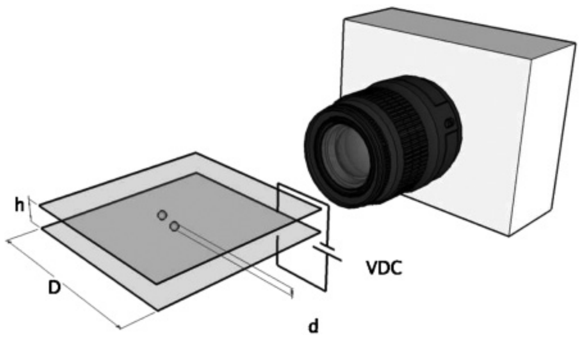

FIG. 1. Sketch of the experimental setup. One or two spherical conducting beads are placed between two horizontal plane electrodes plugged into a high-voltage power supply. A fast CCD camera and a tracking algorithm are used to record the trajectory of the beads.

up to 25 g. Three regions denoted I, II, and III correspond to three dynamical regimes described in Sec. III B.

We measured the period T of the limit cycle of a 488-μm coated glass bead. Figure 4 presents the period T as a function of the applied voltage V. Each dot is an average computed over 20–50 oscillations. As expected from the above observations, the period decreases with increasing voltage.

When a horizontal velocity is given to a bead bouncing on the bottom plate, it keeps a finite horizontal velocity for a long time. In contrast, when a bead bounces alternatively on both plates, it rapidly reaches a quasivertical oscillation. A horizontal stabilization effect occurs for a bead bouncing alternatively on two facing plates (see Fig. 5). The mechanism for this stabilization is not trivial. However, we can understand that when a bead is bouncing between two plates, the moment of the friction force can change the sign at each bounce and tend to reduce the rotation of the bead. This is not the case for a bead bouncing only on the bottom plate.

By drawing a mark on the beads, we could observe their rotation. When a bead is bouncing between two plates with a nonzero horizontal component of velocity, its angular rotation speed is initially on the order of 15 rad/s. During the collisions, the sign of angular rotation can change. After a few collisions, the angular velocity vanishes rapidly. However, when the bead is bouncing on the bottom plate only, the sign of the angular rotation remains unchanged and the angular velocity slowly vanishes.

This effect was already reported by Leconte *et al.* [22] for a bead mechanically shaken between two parallel plates. They took advantage of this to make precise measurements of the normal restitution coefficient of a steel bead. It also plays a crucial role for the experiment described in Sec. IV of this paper.

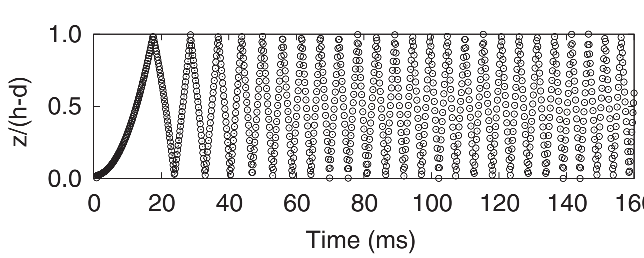

FIG. 2. Temporal evolution of the vertical coordinate z of a single coated glass bead of 488 μm under 2000 V. The vertical coordinate z is normalized by $h-d$ in order to obtain values in the interval [0,1].

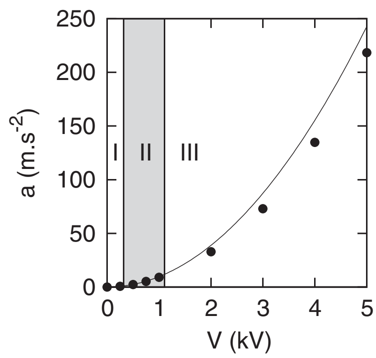

FIG. 3. Measured acceleration a of a coated glass bead of 400 μm. The solid curve represents Eq. (4) without any fitting parameter. Three regions I, II, and III represent three dynamical regimes described in Sec. III B.

B. Mathematical description

In the following we will suppose that the charging time of the conducting bead is shorter than the time of contact with an electrode. This means that the electrostatic equilibrium is reached during each contact. The damping due to viscous friction with air is negligible.

First let us calculate the force F_c that acts on a bead when it is in contact with an electrode. If the diameter d of the bead is small compared to the gap h between the electrodes, we can refer to the problem of a sphere in contact with a plane placed at the same electric potential. According to Maxwell [23], F_c reads

$$F_c = \pi c \epsilon_0 d^2 E_0^2, \tag{1}$$

where ϵ_0 is the vacuum permittivity, $E_0 = V/h$ is the applied electric field, ρ is the density of the bead, d is its diameter, and $c \approx 1.36$ is an integration constant. If this force is larger than the weight of the bead, it cannot stay on the bottom plate and

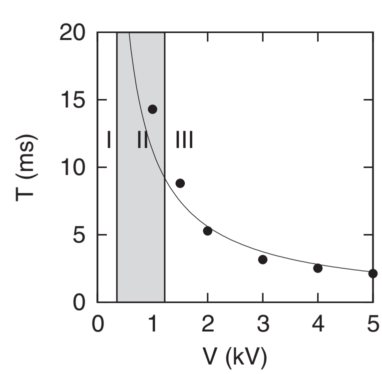

FIG. 4. Measured period T of the limit cycle of a coated glass bead of 488 μm. The solid curve represents Eq. (6) without any fitting parameter. Three regions I, II, and III represent three dynamical regimes described in Sec. III B.

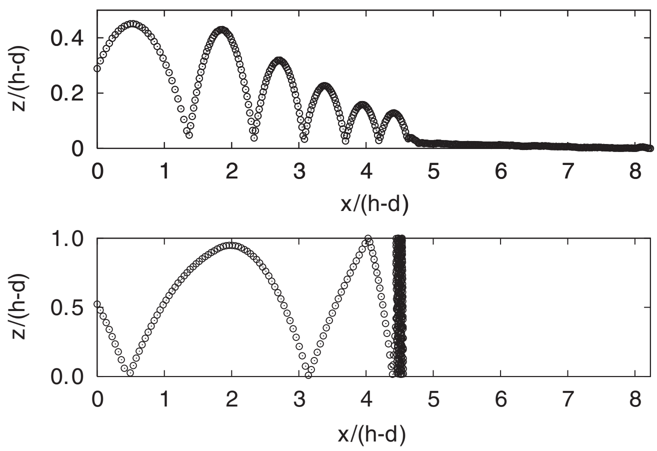

FIG. 5. Horizontal stabilization of a bouncing bead. The horizontal velocity of a bead bouncing on the bottom plate is slowly reduced (top). The horizontal velocity of a bead bouncing between two plates is rapidly reduced and the trajectory becomes quasivertical (bottom). Both pictures correspond to the same bead, to the same applied voltage, and the same video length.

it reaches the limit cycle. The critical electric field E_2 for this force balance is given by

$$E_2 = \left(\frac{\rho g d}{6c\epsilon_0}\right)^{1/2}. \tag{2}$$

This expression was used by Aranson and co-workers and it appears as a critical value on the phase diagrams of several experiments conducted with a large number of particles [11–14]. When the bead accelerates between the electrodes, it experiences an electric force F_a. This force is no longer given by Eq. (1). If the diameter d is small compared to the gap h, we can consider that during the trajectory between the electrodes, the bead is submitted to a force of the form

$$F_a = qE_0,$$

where q is the total charge on the bead. The exact expression of this charge has been calculated in Ref. [23]. We use it to express F_a as

$$F_a = \frac{\pi^3\epsilon_0 d^2 E_0^2}{6} = \frac{\pi^2}{6c}F_c. \tag{3}$$

A more accurate expression of the force acting on a conducting sphere close to a plane electrode can be found in Ref. [24]. The forces F_a and F_c are sketched in Fig. 6. When the bead is going upward, it is submitted to an acceleration $a - g$, where

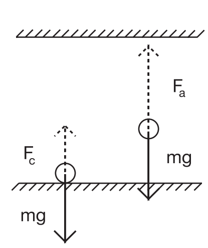

FIG. 6. When a bead is in contact with an electrode, it experiences its weight and a force F_c given by Eq. (1). When it is far from the electrodes, it experiences its weight and an electric force F_a given by Eq. (3).

g is the gravitational acceleration. When it goes downward, it is submitted to an acceleration $-a - g$. The acceleration a due to the force F_a reads

$$a = \frac{\pi^2\epsilon_0 E_0^2}{\rho d}. \tag{4}$$

After several collisions, the bead reaches a periodic limit cycle. During one period of this limit cycle, the energy given by the work of the electric force is counterbalanced by the energy dissipated during the collisions. The period T of the limit cycle can therefore be expressed as

$$T = \left(\frac{\sqrt{2}}{a+g} - \frac{e\sqrt{2}}{a-g}\right)\left(\frac{(h-d)(a+g+ae^2-ge^2)}{1-e^4}\right)^{1/2} + \left(\frac{\sqrt{2}}{a-g} - \frac{e\sqrt{2}}{a+g}\right)\left(\frac{(h-d)(a-g+ae^2+ge^2)}{1-e^4}\right)^{1/2}. \tag{5}$$

If $a \gg g$, T can be expressed as

$$T \approx \frac{\sqrt{8}}{\pi}\left(\frac{1-e}{1+e}\frac{\rho d(h-d)}{\epsilon_0 E_0^2}\right)^{1/2}. \tag{6}$$

The limit cycle can still be stable if $F_c < mg$. There is another critical field E_1 below which the limit cycle becomes unstable. This critical electric field is written

$$E_1 = \left(\frac{1-e^2}{1+e^2}\frac{\rho g d}{\pi^2\epsilon_0}\right)^{1/2} = \left(\frac{1-e^2}{1+e^2}\frac{6c}{\pi^2}\right)^{1/2} E_2. \tag{7}$$

The dynamics of the system is therefore determined by three regimes.

In region I ($E_0 < E_1$), the only stable attractor is a fixed point: The bead stays on the bottom plate.

In region II ($E_1 < E_0 < E_2$), there are two stable attractors: a periodic limit cycle and a fixed point.

In region III ($E_0 > E_2$), the fixed point loses its stability and the limit cycle is the only stable attractor.

The predictions of this model are respectively plotted in Figs. 3 and 4. The acceleration a [Eq. (4)], the period T [Eq. (6)], and the critical electric fields E_1 and E_2 [Eqs. (7) and (2)] are predicted without fitting parameters. We use $\rho = 2500\,\mathrm{kg\,m^{-3}}$, $d = 400\,\mu\mathrm{m}$, and $d = 488\,\mu\mathrm{m}$. The normal restitution coefficient $e = 0.905$ is measured independently. The values E_1 and E_2 are measured for a steel bead of diameter $d = 500\,\mu\mathrm{m}$. The value of E_2 is correctly predicted by Eq. (2). The experimental value of E_1, however, is larger than the one predicted by Eq. (7). When decreasing the electric field above E_1, small fluctuations of the bead velocity may cause the loss of stability of the oscillations. Experiments and theory are in agreement. The small deviations of the master curve in Fig. 4 are probably due to the effect of projection due to the position of the camera.

The dynamics of a single bead electrically shaken is more simple than the dynamics of a bead mechanically shaken between two oscillating plates. Only two attractors are observed for electrical shaking, whereas a bifurcation cascade and chaotic orbits are expected for mechanical shaking [25,26].

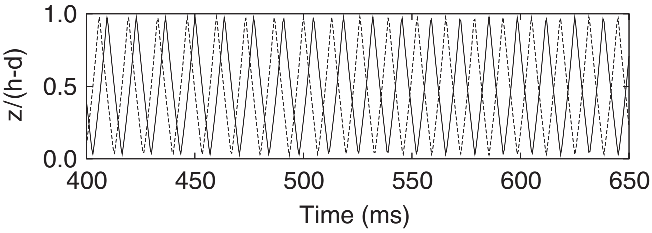

FIG. 7. Temporal evolution of the vertical coordinate of two interacting steel beads of 2 mm diameter under a voltage of 2000 V. The beads oscillate at the same frequency and their phases are in opposition.

IV. DYNAMICS OF SEVERAL INTERACTING BEADS

A. Two beads

In this section we describe the experiment of two neighboring identical beads in a capacitor. The beads are stainless steel beads with a diameter of $d = 2$ mm. The applied voltage V is 2000 V. The frame rate of the video camera is 2000 fps.

Figure 7 shows a typical evolution of the height z of two neighboring beads. The beads oscillate with the same frequency and after few collisions with the plates their phases are in opposition. The horizontal stabilization effect described in Sec. III A is crucial for this experiment: Both beads need to keep a constant frequency and stay close to each other to become antisynchronized.

In order the measure a phase shift between the experimental trajectories of the beads, we defined the following parameter:

$$\phi(t) = \cos^{-1}\left(\frac{\langle[z_1(t)-\bar{z}_1][z_2(t)-\bar{z}_2]\rangle_T}{\sqrt{\langle[z_1(t)-\bar{z}_1]^2\rangle_T\langle[z_2(t)-\bar{z}_2]^2\rangle_T}}\right),$$

where z_i designates the vertical coordinate of the bead i, $i \in \{1,2\}$, $\bar{z}_i$ is the average of z_i over the total length of the video, and the bracket $\langle f(t)\rangle_T$ denotes the mobile average $\int_0^T f(t+\tau)d\tau$ of the function f over one period T.

Figure 8 illustrates the temporal evolution of the phase shift ϕ and the horizontal separation $x_1 - x_2$ between the beads. The total time of the sample shown in this picture (1050 ms) corresponds to 75 oscillations. After some time, ϕ reaches a horizontal plateau, indicating a phase locking at a phase shift of π. When the beads are synchronized, they are attracted to each other and they undergo a collision. After the collision, the separation between the beads is rapidly stabilized and they undergo a second collision. This is the sign of the stabilization effect described in Sec. III A. This behavior is typical for a system of two identical beads. We repeat the measurements of ϕ several times; the horizontal plateau of ϕ is reproducible and it always appears for a phase shift of π.

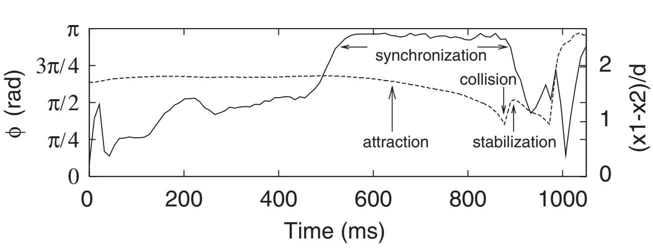

FIG. 8. Typical temporal evolution of the phase shift ϕ (solid line) and horizontal separation $(x_1 - x_2)/d$ (dashed line) for two neighboring beads. A phase synchronization is shown for $\phi = \pi$, during which the beads are attracted to each other. After some time, the beads collide and are stabilized horizontally. The corresponding vertical coordinates z are illustrated in Fig. 7 for the time interval $t \in [400,650]$.

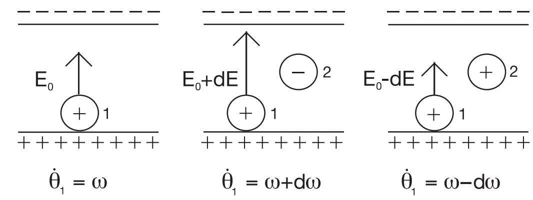

FIG. 9. The local electric field during the charging of a bead is modified by the presence of the other bead. The acquired charge and the further acceleration of this bead depend on the phase of the other bead.

B. Mathematical description

We propose a simple mechanism for the antiphase synchronization described in the preceding section. Let us consider two beads 1 and 2 and define two phases θ_1 and θ_2 by $\cos\theta_i = 1 - \frac{2z_i}{h-d}$, $i \in \{1,2\}$. Let us suppose that, without interaction, we have $\dot{\theta_1} = \dot{\theta_2} = \omega$. When the beads are close to each other, they interact electrostatically. We know that the charge acquired by a bead in contact with an electrode is proportional to the electric field. We also know that after the detachment, the acceleration of the bead is proportional to its charge. When two beads are close to each other, the local electric field is modified by the presence of the other bead. The charge acquired by a bead during contact therefore depends on the phase of the other bead. This mechanism is illustrated in Fig. 9.

By considering the sign of the variation of the local electric field for several values of θ_1 and θ_2, we can write an expression that qualitatively describes the evolution of the phase of the interacting beads. This gives the following Kuramoto-like equations:

$$\begin{aligned}\dot{\theta_1} &= \omega + K(\beta - \cos\theta_1 \sin\theta_2)\\ \dot{\theta_2} &= \omega + K(\beta - \cos\theta_2 \sin\theta_1),\end{aligned} \tag{8}$$

where K and β are two positive coupling constants. From this expression, we can deduce an equation of evolution for the phase shift $\phi = \theta_1 - \theta_2$:

$$\dot{\phi} = K \sin(\phi). \tag{9}$$

The only stable stationary solution of this equation implies

$$\phi = (2k+1)\pi, \tag{10}$$

where k is an integer. This minimalist Kuramoto-like model predicts some synchronization effect. Only an antiphase situation is predicted, as observed experimentally.

C. Three beads

We perform experiments on a set of three beads aligned or arranged in a triangle. Only a partial synchronization is

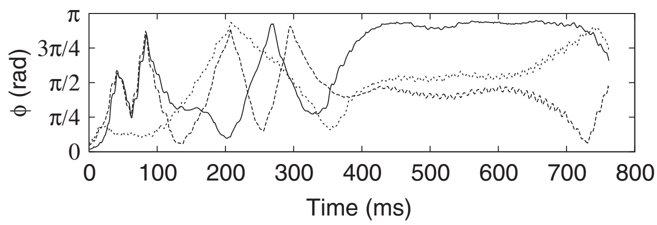

FIG. 10. Temporal evolution of the phase shifts ϕ between the pairs of beads in a configuration of three aligned beads. One could observe a partial synchronization for $\phi = \pi$ for a pair of beads (solid curve) while the other beads (dashed curves) are not synchronized.

observed: Two beads could synchronize with a phase shift of π, similarly to Sec. IV A, while the phase shift between the other couples of beads fluctuates (see Fig. 10).

Experiments with more than two beads are not obvious since the interdistance should be finely controlled in order to induce interactions between the bodies. When more than two beads are present, synchronization appears only for couples of neighboring objects. Since beads are freely moving, reorganization destroys any ordered pattern. This effect could play a major role in the collective motion of beads in between two plates. The investigation of these collective effects for many beads, however, is beyond the scope of the present paper.

V. CONCLUSION

We performed several experiments concerning the dynamics of spherical conducting particles in a plane capacitor. For a single bead, there are two stable attractors: The bead can stay on the bottom electrode or bounce periodically between both electrodes. The acceleration of the bead and the period of its limit cycle were measured as a function of the applied voltage. We propose a zero-fitting parameter model that is in agreement with the experiments. This model also predicts the stability limits for both attractors. Moreover, a horizontal stabilization effect is observed: A bead bouncing between two electrodes tends to reach a quasivertical trajectory, whatever its initial horizontal velocity. Thanks to this effect, when two identical beads are placed together in a capacitor, an antiphase synchronization can be observed. We suggest that this synchronization is due to the modification of the local electric field during the charging of the beads. A Kuramoto-like model is proposed, which represents a basis for further studies.

ACKNOWLEDGMENTS

This work has been supported by INANOMAT project (Grant No. IAP P6/17) of the Belgian Science Policy. We acknowledge J.-C. Remy, F. Bochini, R. Cloots, G. Lumay, and F. Ludewig for help and fruitful discussions.

[1] A. Khayari, A. T. Pérez, and A. Castellanos, in *The Charge Acquired by a Spherical Ball Bouncing on an Electrode: Comparison between Theory and Experiment*, edited by World Scientific Publishing Company, 2000 Annual Report Conference on Electrical Insulation and Dielectric Phenomena, Vol. 2 (IEEE, Piscataway, NJ, 2002), p. 470.

[2] C. Soria, A. Ramoz, and A. T. Pérez, Europhys. Lett. **37**, 541 (1997).

[3] M. Saint Jean, C. Even, and C. Guthmann, Europhys. Lett. **55**, 45 (2001).

[4] M. Saint Jean and C. Guthmann, J. Phys. Condens. Matter **14**, 13653 (2002).

[5] M. Saint Jean, C. Guthmann, and G. Coupier, Eur. Phys. J. B **39**, 61 (2004).

[6] G. Coupier, C. Guthmann, Y. Noat, and M. Saint Jean, Phys. Rev. E **71**, 046105 (2005).

[7] P. Galatola, G. Coupier, M. Saint Jean, J.-B. Fournier, and C. Guthmann, Eur. Phys. J. B **50**, 549 (2006).

[8] G. Coupier, M. Saint Jean, and C. Guthmann, Europhys. Lett. **77**, 60001 (2007).

[9] C. Coste, J.-B. Delfau, C. Even, and M. Saint Jean, Phys. Rev. E **81**, 051201 (2010).

[10] J.-B. Delfau, C. Coste, C. Even, and M. Saint Jean, Phys. Rev. E **82**, 031201 (2010).

[11] I. S. Aranson, D. Blair, V. A. Kalatsky, G. W. Crabtree, W.-K. Kwok, V. M. Vinokur, and U. Welp, Phys. Rev. Lett. **84**, 3306 (2000).

[12] D. W. Howell, I. S. Aronson, and G. W. Crabtree, Phys. Rev. E **63**, 050301(R) (2001).

[13] I. S. Aranson, B. Meerson, P. V. Sasorov, and V. M. Vinokur, Phys. Rev. Lett. **88**, 204301 (2002).

[14] M. V. Sapozhnikov, I. S. Aranson, and J. S. Olafsen, Phys. Rev. E **67**, 010302(R) (2003).

[15] M. V. Sapozhnikov, A. Peleg, B. Meerson, I. S. Aranson, and K. L. Kohlstedt, Phys. Rev. E **71**, 011307 (2005).

[16] I. S. Aranson and J. S. Olafsen, Phys. Rev. E **66**, 061302 (2002).

[17] M. V. Sapozhnikov, Y. V. Tolmachev, I. S. Aranson, and W.-K. Kwok, Phys. Rev. Lett. **90**, 114301 (2003).

[18] I. S. Aranson and M. V. Sapozhnikov, Phys. Rev. Lett. **92**, 234301 (2004).

[19] M. V. Sapozhnikov, I. S. Aranson, W.-K. Kwok, and Y. V. Tolmachev, Phys. Rev. Lett. **93**, 084502 (2004).

[20] K.-Q. Zhang and X. Y. Liu, J. Chem. Phys. **130**, 184901 (2009).

[21] N. Vandewalle, G. Lumay, F. Ludewig, and J. E. Fiscina (unpublished).

[22] M. Leconte, Y. Garrabos, F. Palencia, C. Lecoutre, P. Evesque, and D. Beysens, Appl. Phys. Lett. **89**, 243518 (2006).

[23] J. C. Maxwell, in *A Treatise on Electricity and Magnetism*, Vol. I (Dover, New York, 1891), pp. 268–276.

[24] A. T. Pérez, J. Electrostat. **56**, 199 (2002).

[25] T. Gilet, N. Vandewalle, and S. Dorbolo, Phys. Rev. E **79**, 055201(R) (2009).

[26] N. Vandewalle, T. Gilet, and S. Dorbolo (unpublished).